

Mechanistic study of ethanol conversion into butadiene over silver promoted zirconia catalysts

Vitaly L. Sushkevich ^{a,b,*}, Irina I. Ivanova ^{a,b}

^a Department of Chemistry, Lomonosov Moscow State University, Leninskie Gory 1, Bld. 3, 119991 Moscow, Russia

^b ETB Cat LLC, Leninskie Gory 1, bld. 75 v, 119991 Moscow, Russia

ARTICLE INFO

Article history:

Received 10 January 2017

Received in revised form 15 May 2017

Accepted 20 May 2017

Available online 22 May 2017

Keywords:

Kinetic analysis
Deuterium tracing
Mechanism
Ethanol
Butadiene

ABSTRACT

Combined application of kinetic measurements, SSITKA and deuterium tracing techniques allowed to elucidate the mechanism of the key steps of butadiene synthesis over silver promoted zirconia catalysts, including ethanol dehydrogenation, acetaldehyde aldol condensation, and crotonaldehyde reduction with ethanol, and to determine the rate-limiting step of the process. We show for the first time that butadiene synthesis involves two independent catalytic cycles: i) dehydrogenation of ethanol into acetaldehyde over metal sites, and ii) acetaldehyde/ethanol transformation into butadiene over Lewis acidic sites. The first cycle implies ethanol dehydrogenation into acetaldehyde via concerted cleavage of CH₂ and OH groups, followed by the fast desorption of the products formed into the gaseous phase. The second cycle starts with the activation of acetaldehyde over Lewis acid sites through enolization and its interaction with another acetaldehyde molecule from the gaseous phase via Eley-Rideal mechanism. The formed 3-hydroxybutanal further dehydrates into crotonaldehyde. The aldol condensation step was proposed to be rate-determining. Further transformation of crotonaldehyde proceeds through Langmuir-Hinshelwood mechanism, involving the interaction of crotonaldehyde with ethanol over a Lewis site via a six-member ring transition state. Subsequently, crotyl alcohol dehydrates into butadiene, and acetaldehyde adsorbed over Lewis sites initiates the next catalytic cycle. The proposed molecular-level mechanism gives insights into rational design of efficient catalysts for the ethanol conversion into butadiene.

© 2017 Elsevier B.V. All rights reserved.

1. Introduction

Production of chemicals from renewable feedstocks attracts a lot of interest, since efficient technologies can be easily embedded into the existing industrial infrastructure. In addition, synthesis of chemicals from bio-based sources is economically preferable compared to the production of fuels [1]. Various molecules were considered as potential building blocks for the synthesis of basic chemicals; however only few, including ethanol, could be easily introduced into existing industrial processes [2,3].

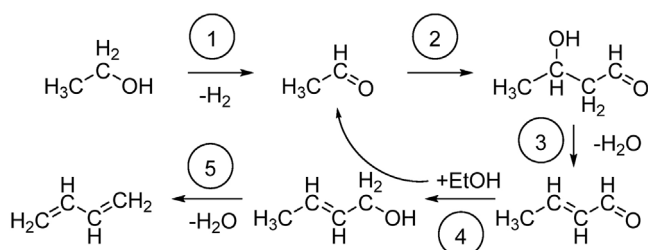
Over the past decade, applications of ethanol as a starting chemical have initiated a new wave of interest because of economic benefits seen in bioethanol feedstock [2–5]. The highest profit could be achieved for the ethanol transformation into butadiene, which is one of the most important building blocks for the production of wide variety of synthetic rubbers, elastomers and resins [4–6].

About 95% of butadiene is currently obtained as a by-product of the ethylene and propylene production via the hydrocarbons steam cracking. Isolation of butadiene from the other products requires a number of expensive extractive distillation steps [7]. The predicted shift towards lighter feedstocks for steam cracking due to the recent shale gas revolution will lead to a significant decrease of butadiene production yield, and will affect its market price significantly. As such, efficient on-purpose butadiene synthesis technologies are highly desirable. [1–7]

These issues generated a new wave of interest in the ethanol-to-butadiene process and several groups significantly contributed to the design of novel catalysts with remarkable activity and selectivity [8–31]. However, although significant achievements have been made towards the development of novel efficient catalysts, there is still need for fundamental understanding of the process and its mechanism. Various reaction schemes and different rate-determining steps were reported for the ethanol transformation into butadiene over different catalytic systems. For more information the reader is referred to the recent review papers by Angelic et al. [2] and Makshina et al. [3].

* Corresponding author at: Lomonosov Moscow State University, Chemistry Department, Leninskye Gory, 1-3, 119991 Moscow, Russia.

E-mail address: vitaly.sushkevich@psi.ch (V.L. Sushkevich).

**Scheme 1.** Main reaction pathway leading to butadiene.

Originally, Lebedev et al. suggested the radical mechanism for the butadiene formation from ethanol [32]. Acetaldehyde was identified as a primary reaction product, while butadiene was assumed to be tertiary product. Later, Balandin concluded that the butadiene synthesis proceeds through the formation of 1,3-butanediol [33]. This reaction pathway was similar to the mechanism proposed earlier by Ostromyslensky for two-step butadiene synthesis using the mixture of ethanol with acetaldehyde as a feedstock [34]. However, the detailed investigation of the transformation of various reactants led to the conclusion that both Lebedev and Ostromyslensky processes proceeded via an intermediate formation of crotonaldehyde. [35–39] Finally, the suggested reaction pathway included the formation of acetaldol via the aldol condensation of two acetaldehyde molecules, followed by its dehydration into crotonaldehyde. The key role of crotonaldehyde as the intermediate product was further confirmed by Vinogradova et al. by using ^{14}C labeled acetaldehyde. [40] Now it is generally assumed that this C–C coupling reaction is responsible for the butadiene C₄ chain formation.

Further transformation of crotonaldehyde into butadiene has been debated for a long time. Quattlebaum et al. [37] suggested that crotonaldehyde undergoes reduction with ethanol. Based on thermodynamic calculations, Natta and Rigamonti [38], and later Bhattacharyya and Sanyal [39], confirmed that the formation of butadiene can proceed via the reduction of crotonaldehyde with ethanol, yielding crotyl alcohol. The direct reduction of crotonaldehyde by hydrogen was shown to be thermodynamically unfavorable. Later, Niiyama et al. postulated for the first time that the reduction of crotonaldehyde with ethanol proceeds via Meerwein–Ponndorf–Verley–Oppenauer mechanism (MPVO). The generally accepted reaction route, is shown in **Scheme 1**.

An alternative reaction pathway proposed by Gruver et al. [43] involves interaction between acetaldehyde and ethylene via the Prins reaction. From the thermodynamic point of view, the Prins mechanism is possible; however, it is less favorable than the aldol condensation pathway. Notwithstanding, no experimental evidences confirming the Prins mechanism have been provided so far.

Although the overall reaction route leading to butadiene is now firmly established, the rate-limiting step is still the subject of debate. Natta et al. [38] and Bhattacharyya et al. [39] proposed that aldol condensation step is the rate-determining step over the Al₂O₃/ZnO catalysts. For the basic mixed MgO/SiO₂ oxide catalysts Niiyama et al. assumed that ethanol dehydrogenation is the rate-limiting step [41]. In contrast to Niiyama work, Kvise et al. suggested the acetaldehyde condensation to be rate-determining over the magnesia catalyst, rather than the dehydrogenation of ethanol to acetaldehyde [42]. In our recent work [8–10,44,45] we have demonstrated that doping of oxide catalysts with the small amount of metals leads to a significant acceleration of the dehydrogenation step, which renders aldol condensation rate-determining.

It should be noted that most of the mechanistic studies published so far are focused at the determination of the main reaction steps and the reaction network. The detailed information on the mechanisms of each reaction step is still not available. At the same

time, this information is crucial for understanding of the process and for further improvement of the catalysts.

In this original contribution we aim at the deeper insight into the mechanism of the key steps of ethanol conversion into butadiene over model zirconia catalyst doped with Ag. The combined application of various techniques including kinetic studies, SSITKA measurements and isotope tracing experiments used for this reaction first time allowed to determine the kinetic isotope effects, residence times and isotopic label distribution in various products and intermediates, and to discriminate between the Langmuir–Hinshelwood and Eley–Rideal mechanisms of different reaction steps. Based on these results, for the first time a detailed molecular-level mechanism of ethanol conversion into butadiene including two independent catalytic cycles was proposed for metal promoted Lewis acid catalysts. Discovering those independent catalytic cycles opens new principal opportunities for the rational catalyst design and reaction conditions optimization for the further industrial implementation of the process.

2. Experimental

2.1. Catalysts preparation

Silver promoted and silver free catalysts were prepared by incipient wetness impregnation of silica gel (supplied by Karpov Chemical Plant) with aqueous solutions of AgNO₃ and ZrO(NO₃)₂ to reach silver and zirconia loading of 1 and 4 wt%, respectively. The solutions of silver and zirconyl nitrates were prepared by gradual dissolutions of corresponding salts in distilled water at 323 K under stirring until the clear solution was obtained (ca. 1 h). For silver and zirconium-containing sample the impregnation was done in one step. Immediately after the preparation, the solution was used for impregnation of 0.25–0.5 mm fraction of silica gel. After impregnation, the sample was dried overnight at ambient temperature, then at 383 K for 3 h, heated in a flow of dry air to 873 K with the temperature ramp of 2 K/min and calcined at this temperature during 4 h. Catalysts were denoted as Ag/ZrO₂/SiO₂ and ZrO₂/SiO₂.

2.2. Catalysts characterization

The elemental analysis was performed using energy dispersive X-ray fluorescence spectroscopy (EDXRF). Prior to the analysis the samples were mixed with B(OH)₃ and pressed in self-supporting wafers. The wafers were analyzed using a Thermo Scientific ARL Perform'x WDXRF. N₂ sorption-desorption isotherms were measured at 77 K using a Micromeritics 2000 automatic surface area and pore size analyzer. These data along with acidity and TEM measurements are given in Supporting Information.

2.3. Kinetic analysis and deuterium tracing

Catalytic experiments on ethanol transformation into butadiene were carried out in a flow-type fixed-bed reactor under the atmospheric pressure. In a typical experiment, 1 g of catalyst (fraction 0.25–0.5 mm) was packed into the quartz tubular reactor between two quartz wafers and purged with nitrogen at 673 K for 0.5 h with subsequent reduction of silver in a flow of hydrogen for 0.5 h at 600 K. For silver promoted catalyst pure ethanol was used as a feed while for silver free catalyst acetaldehyde or crotonaldehyde was added to ethanol.

Acetaldehyde and crotonaldehyde was fed using saturator, which was kept at 273 K in an ice bath. Ethanol was fed by a Razel syringe pump. Helium was used as a carrier gas, the partial pressures of ethanol and acetaldehyde were varied from 0.00 to 0.82 bar and from 0.00 to 0.45 bar, respectively.

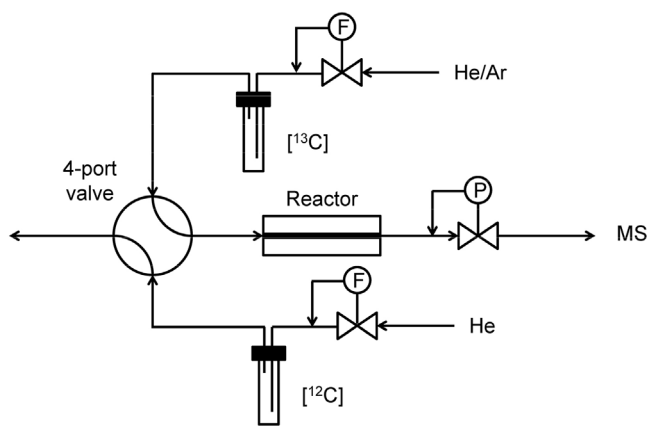


Fig. 1. Schematic representation of reaction system for SSITKA.

For D-tracing experiments, unlabeled ethanol $\text{CH}_3\text{CH}_2\text{OH}$ as well as deuterium labeled $\text{CH}_3\text{CD}_2\text{OH}$, $\text{CD}_3\text{CH}_2\text{OH}$, $\text{CH}_3\text{CH}_2\text{OD}$ and $\text{CD}_3\text{CD}_2\text{OD}$ (Cambridge Isotopes Laboratories, Inc.) reagents were fed using a saturator, which was kept at 298 K. Helium was used as a carrier gas (molar ratio EtOH/He = 20). The WHSV was kept 0.3 h^{-1} , the reaction temperature was 600 K. The reaction products were absorbed by the CDCl_3 solution kept in an ice bath.

Methane was used as an unreactive internal standard in order to ensure good mass balances. All products were analyzed online using Crystal 2000 M gas chromatograph using 50 m SE-30 column. The rates of acetaldehyde and butadiene formation were calculated as follows:

$$R_i = F_{\text{CH}_4} \frac{m_i}{m_{\text{CH}_4}} \frac{16}{M_r} \frac{1}{M_{\text{cat}}}$$

where F_{CH_4} —methane flow, mmol h^{-1} , m_i – mass of i-product in reaction mixture, M_r – molecular weight of i-product, M_{cat} – mass of the catalyst.

^1H NMR and GC-MS were used to elucidate the fractions and chemical structure of butadiene isotopomers formed in the reaction. For GC-MS analysis Thermo Scientific Trace chromatograph equipped with DSQII mass detector was used. ^1H NMR spectra were recorded with a Bruker AVANCE 600 spectrometer (600.12 MHz) for samples dissolved in CDCl_3 . Chemical shifts are given in ppm relative to SiMe_4 .

2.4. SSITKA

A schematic representation of the SSITKA system is shown in Fig. 1. After achieving steady-state ethanol conversion (ca. 1 h on stream), isotopic switch was performed using a two-position valve, from unlabeled ^{12}C ethanol (anhydrous, Sigma-Aldrich; 99.5%) to CH_2 labeled ethanol- $^{13}\text{C}_1$ (Cambridge Isotopes Laboratories, Inc.; 1- ^{13}C , 99%). For some experiments, unlabeled and labeled (Cambridge Isotopes Laboratories, Inc.; 1,2- ^{13}C , 98%) acetaldehyde was used. The unlabeled/labeled reagents were each contained in two saturators that were kept together in a temperature-controlled water bath. Helium was used as the carrier gas and flowed through the saturators giving ~6% volume fraction of ethanol or acetaldehyde in the gas phase. The ^{13}C labeled reagents gas feed was mixed with an inert argon tracer (5 vol% of the total flow rate) that was used to correct for the gas-phase holdup in the reactor. The SSITKA experiments were carried out at constant total gas flow rates of $35 \text{ cm}^3 \text{ min}^{-1}$. The $^{12}\text{C}/^{13}\text{C}$ switch was achieved without perturbing the steady-state of the reaction by maintaining the reaction temperature at 600 K, the total system pressure at 1 atm and ethanol conversion at 5%. On-line mass spectrometry analysis was performed by RGA200 mass analyzer (Stanford Research Systems).

In the MS, the ion signals for $m/z=40$ (Ar tracer), 29–32, 39, 41, 43–46, and 53–56 were continuously monitored to determine the isotope content of the original gas sample. Due to the overlapping, MS signals were corrected basing on MS responses obtained for pure ethanol, acetaldehyde and butadiene passed through the SSITKA reactor without the catalyst. We used linear combination fitting (LCF) with ordinary least squares (LCF) optimization and intensity ratios for pure compounds to estimate the fractions of $\text{CH}_3^{12}\text{CHO}$, $\text{CH}_3^{13}\text{CHO}$, $\text{CH}_3^{12}\text{CH}_2\text{OH}$, $\text{CH}_3^{13}\text{CH}_2\text{OH}$ and butadiene with 0, 1 and 2 ^{13}C atoms. Due to the high selectivity of the reaction, the impact of by-products into the final SSITKA data was negligible.

Transient responses were normalized by the difference between the initial and final ion signals. The argon decay curve was used to determine the gas-phase holdup of the reactor system, since we assumed that the inert gas did not adsorb on the surface of the catalyst. Therefore, the difference in area under the normalized transient response of each species (F_i) from that of the inert Ar tracer (F_{Ar}) is equal to the overall mean surface residence time of that species (τ_i):

$$\tau_i = \int_0^N (F_i(t) - F_{\text{Ar}}(t)) dt$$

3. Results

To access the mechanism of complex reactions involving several consecutive steps, a combination of various techniques is usually required. In this contribution we applied kinetic measurements, SSITKA studies, and isotopic label tracing to get deeper insight into the mechanisms of the key steps of the ethanol conversion into butadiene, namely, ethanol dehydrogenation, acetaldehyde condensation, and crotonaldehyde reduction. The experiments were carried out using unlabeled ethanol and ethanol/acetaldehyde mixtures and specifically labeled compounds. Deuterated compounds including $\text{CD}_3\text{CH}_2\text{OH}$, $\text{CH}_3\text{CD}_2\text{OH}$, $\text{CH}_3\text{CH}_2\text{OD}$ and $\text{CD}_3\text{CD}_2\text{OD}$ were used for the investigation of kinetic isotope effects and tracing of deuterium label in intermediates and products, ethanol- $^{13}\text{C}_1$ and acetaldehyde- $^{13}\text{C}_2$ were applied in SSITKA measurements for the determination of residence times and normalized responses of reactants and products.

3.1. Kinetic study of ethanol and ethanol/acetaldehyde mixture transformation

Kinetic evaluation of ethanol transformation over $\text{Ag/ZrO}_2/\text{SiO}_2$ catalyst was carried out under varied partial pressures of ethanol at constant total gas flow rate through the catalyst bed. Acetaldehyde and butadiene were found to be the main products of the reaction, with total selectivity towards butadiene and acetaldehyde above 75% and 10% in all experiments, respectively. Besides acetaldehyde and butadiene, the formation of small amounts of ethylene, propylene, linear butenes, diethyl ether, 1-butanol, ethyl acetate and C_6^+ compounds was observed [8].

The increase of the ethanol pressure in the reaction mixture leads to the increase of the rates of the acetaldehyde and butadiene formation (Fig. 2). While the acetaldehyde formation rate is a linear function of the ethanol partial pressure, the butadiene formation rate reveals the deceleration of the reaction at high ethanol pressures, which could be attributed to the saturation of active sites responsible for rate-limiting step with ethanol.

To better understand the reasons of this deceleration, the reaction kinetics was studied over silver-free catalyst in the presence of acetaldehyde or crotonaldehyde added into the reaction feed.

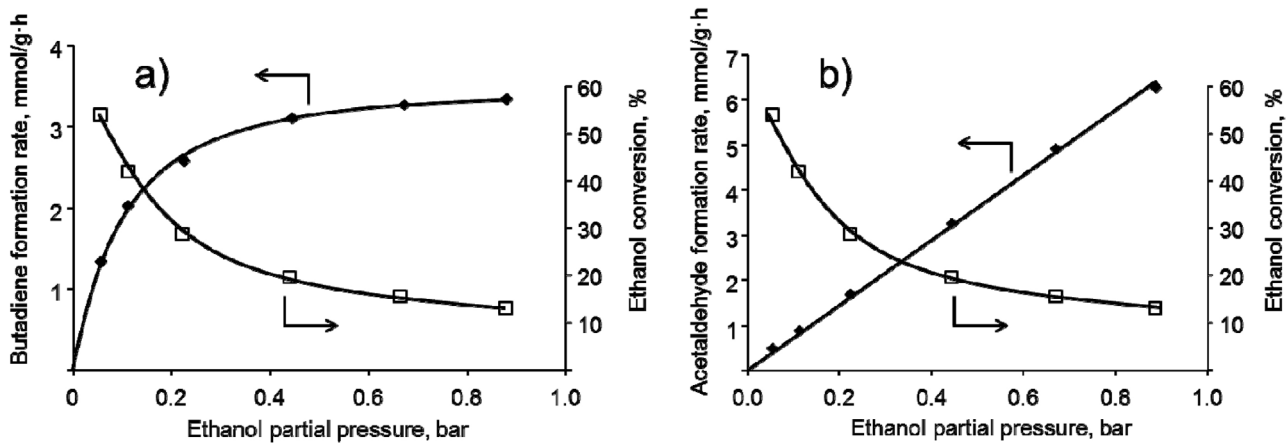


Fig. 2. Butadiene (a) and acetaldehyde (b) formation rates and ethanol conversion versus ethanol partial pressure over $\text{Ag}/\text{ZrO}_2/\text{SiO}_2$ catalyst. $T = 600 \text{ K}$.

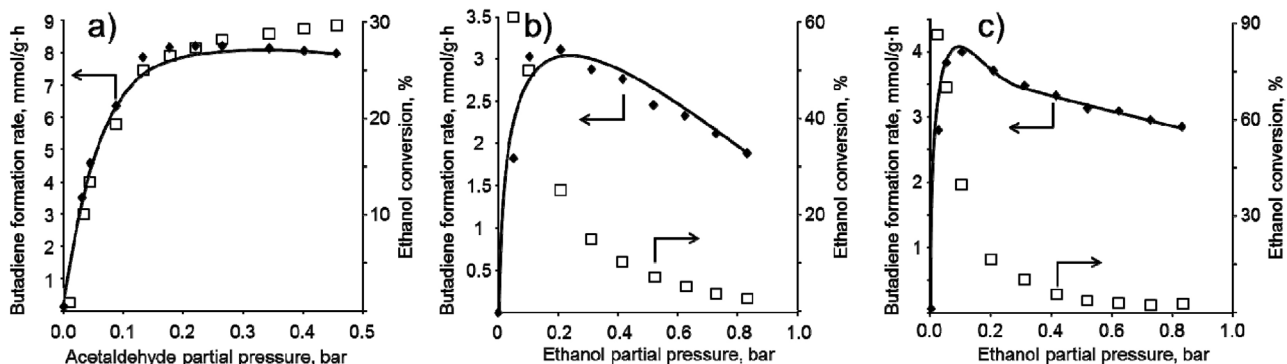


Fig. 3. Butadiene formation rate and ethanol conversion over $\text{ZrO}_2/\text{SiO}_2$ catalyst versus a) acetaldehyde partial pressure at $P_{\text{ethanol}} = 0.4 \text{ bar}$; b) ethanol partial pressure at $P_{\text{acetaldehyde}} = 0.05 \text{ bar}$ and c) $P_{\text{crotonaldehyde}} = 0.03 \text{ bar}$ $T = 600 \text{ K}$.

It should be noticed, that the acidic properties (Fig. S4) and dehydration activity (Table S1) of $\text{Ag}/\text{ZrO}_2/\text{SiO}_2$ and $\text{ZrO}_2/\text{SiO}_2$ catalysts are similar enabling the comparison of the results obtained for both samples studied. The results of ethanol/acetaldehyde mixture transformation at constant ethanol partial pressure of 0.4 bar are shown in Fig. 3a. The increase of acetaldehyde partial pressure from 0.0 to 0.2 bar leads to fast increase of the butadiene formation rate, but further increase of acetaldehyde pressure does not significantly affect the reaction rate indicating the saturation of active sites involved in acetaldehyde transformation.

Variation of ethanol partial pressure at constant acetaldehyde pressure reveals the maximum on the butadiene formation rate curve at ca. 0.2 bar (Fig. 3b). Decrease of the butadiene formation rate at the ethanol pressures higher than 0.2 bar is due to the competitive adsorption of ethanol over the sites occupied by acetaldehyde. Similar results are observed for the ethanol partial pressure variation at the constant crotonaldehyde partial pressure (Fig. 3c), indicating that the interaction of these molecules proceeds over the same sites.

3.2. Kinetic isotope effects observed for specifically labeled ethanol with deuterium

Substitution of H atoms with deuterium in ethanol feed may lead to the kinetic isotope effect (KIE), if during the reaction the C–H cleavage is observed. To estimate the KIE of ethanol transformation, initial rates of the ethanol conversion and the formation of acetaldehyde and butadiene were calculated for the experiments with ethanol deuterated in different positions (Table 1). Here and

below the KIE discussed in the text and given in Table 1 was calculated as follows:

$$KIE = \frac{r_{\text{ethanol isotopologue consumption}}}{r_{\text{C}_2\text{H}_5\text{OH consumption}}} \quad \text{where } r \text{ corresponds to the reaction rate.}$$

It is important to notice that all measurements of reaction rates were carried out after the achievement of the steady state in the terms of ethanol conversion, selectivity and composition of the isotopologues of the products.

For unlabeled ethanol the highest reaction rates are observed, while for all D-labeled ethanol the rates of acetaldehyde and butadiene formation are lower, pointing to the kinetic isotope effects.

For $\text{CH}_3\text{CH}_2\text{OD}$ labeled ethanol acetaldehyde formation rate value is $0.88 \text{ mmol g}^{-1} \text{ h}^{-1}$. The effect could be explained by the participation of OD-groups of ethanol in the dehydrogenation reaction. For $\text{CH}_3\text{CD}_2\text{OH}$ the effect is even higher ($0.72 \text{ mmol g}^{-1} \text{ h}^{-1}$). Completely deuterated ethanol shows the lowest acetaldehyde formation rate. On the contrary, $\text{CD}_3\text{CH}_2\text{OH}$ isotopomer demonstrates only slight difference in acetaldehyde formation rate with respect to unlabeled ethanol, suggesting that the CD_3 groups do not participate in the ethanol dehydrogenation (Table 1).

Among the desorption into gas phase, acetaldehyde can undergo the further transformation into butadiene. Since differently labeled ethanol molecules exhibit different acetaldehyde formation rates, it can be expected that this influences the rates of butadiene formation according to the law of mass action. To subtract the impact of this effect, the ratio of butadiene formation rates to acetaldehyde formation rates was calculated and analyzed (Table 1). The lowest butadiene/acetaldehyde formation ratio (0.62) is observed for $\text{CD}_3\text{CH}_2\text{OH}$. This value is close to those found for fully D-

Table 1

Initial rates of ethanol transformation, acetaldehyde and butadiene formation over Ag/ZrO₂/SiO₂ catalyst (600 K, WHVS = 0.3 h⁻¹, TOS = 30 min).

Initial rates, mmol g ⁻¹ h ⁻¹	CH ₃ CH ₂ OH	CD ₃ CD ₂ OD	CH ₃ CH ₂ OD	CH ₃ CD ₂ OH	CD ₃ CH ₂ OH
Ethanol conversion, %	19.0	7.8	14.7	11.8	13.9
Acetaldehyde formation	1.10	0.57	0.88	0.72	1.03
Butadiene formation	0.97	0.34	0.73	0.58	0.64
Ethanol consumption	3.79	1.56	2.93	2.35	2.77
Butadiene/acetaldehyde formation rate ratio	0.88	0.59	0.83	0.81	0.62
Kinetic isotope effect ^a	–	2.42	1.29	1.61	1.37

^a Calculated as the ratio of ethanol isotopomer consumption rate to the CH₃CH₂OH consumption rate.

Table 2

Residence times estimated for ethanol, acetaldehyde and butadiene at WHSV = 0.46 h⁻¹ and corrected to readsorption effect for Ag/ZrO₂/SiO₂ catalyst.

	Residence time, s	Corrected to readsorption residence time, s
Ethanol	36.7	19.5
Acetaldehyde	33.3	16.5
Butadiene	5.2	0.2

labeled ethanol. This clearly indicates that the C-D cleavage of the CD₃ group significantly influences the rate of the acetaldehyde transformation into butadiene. For CH₃CH₂OD and CH₃CD₂OH the butadiene/acetaldehyde formation ratio is only slightly lower than those observed for the unlabeled ethanol.

The analysis of the overall KIE points that the highest value of 2.42 is observed for CD₃CD₂OD (**Table 1**). For the specifically labeled ethanol compounds the KIE increases in the following order: CH₃CH₂OD < CD₃CH₂OH < CH₃CD₂OH. The results suggest that OD-cleavage is involved only in acetaldehyde formation, the CD₃-cleavage participates mostly in the butadiene formation from acetaldehyde, whereas the CD₂-cleavage can take part in both reactions. The lowest KIE value observed for CH₃CH₂OD confirms that ethanol dehydrogenation is not the rate-determining step of the reaction over Ag/ZrO₂/SiO₂ catalyst.

3.3. SSITKA

SSITKA measurements during the ethanol transformation over Ag/ZrO₂/SiO₂ allow to quantify such kinetic parameters of the reaction as mean surface residence times of adsorbed species (τ), and normalized responses of the reactants and products. [46] In this report we circumscribe the qualitative interpretation of SSITKA results like successfully reported by Davis [46].

Fig. 4 shows the typical SSITKA normalized responses during the feed switch from EtOH-¹³C₁/He/Ar to EtOH-¹²C₂/He mixtures. Argon tracer used for the correction of SSITKA results to system hold-up has a small time constant, which allows analysing the kinetic parameters. Ethanol-¹³C₁ and acetaldehyde-¹³C₁ demonstrate slow transient response, which implies strong interaction with the catalyst surface, while butadiene-¹³C₂ response is much faster. The average surface residence times of ethanol, acetaldehyde and butadiene on Ag/ZrO₂/SiO₂ catalyst are summarized in **Table 2**. Ethanol and acetaldehyde show close residence times of ca. 35 s, while butadiene residence time is much lower (5 s).

Slow decay of ethanol could be associated with its strong adsorption on the surface silanols and further readsorption following the isotope front flow. [47] Such a strong ethanol adsorption was confirmed by SSITKA over pure silica support (Fig. S6), however, the adsorption over Lewis acid sites can not be fully excluded. Therefore, acetaldehyde formed from ethanol adsorbed over catalyst also shows slow decay, which repeats the ethanol response. The easiest method to assess the real surface residence time when readsorption occurs is to carry out the reaction under different contact times and to extrapolate to a value of zero residence time (Fig. S1). Corrected residence times are given in **Table 2**. In the case of

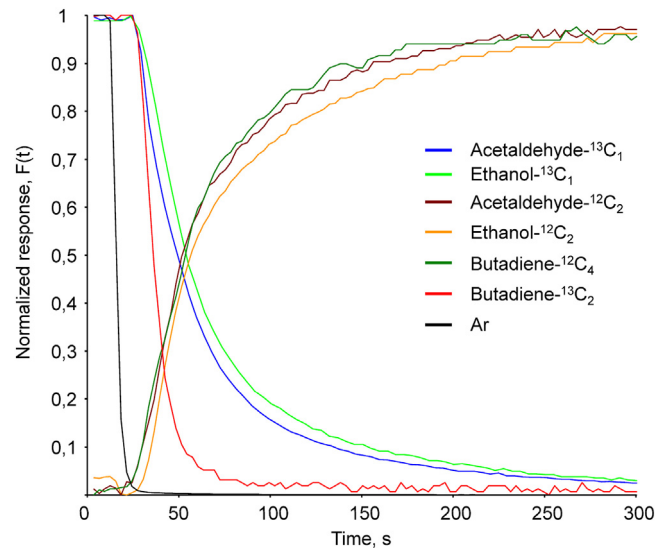


Fig. 4. Normalized isotopic transient response curves following the switch from ethanol-¹³C₁ to ethanol-¹²C₁ with a total flow of 35 cm³ min⁻¹ at 600 K during the reaction of ethanol over Ag/ZrO₂/SiO₂ catalyst.

butadiene, the corrected residence time value is 0.2 s, indicating the absence of any significant interaction with the surface of the catalyst and pointing to the fast reaction rate of butadiene formation. On the contrary, ethanol shows significant impact of readsorption in time response. Acetaldehyde corrected residence time is very close to those calculated for ethanol (**Table 2**).

It should be noted that normalized concentration of double-labeled butadiene-¹³C₂ decays much faster in comparison with evolution of unlabeled butadiene (**Fig. 4**). The responses of unlabeled and labeled butadiene in EtOH-³C₁/He/Ar to EtOH/He and vice versa switches corrected to the system hold-up are shown in **Fig. 5**. The results clearly indicate the fast evolution of the normalized response of butadiene containing one and two ¹³C labels. At the same time, the completely unlabeled butadiene response is much slower. It could be suggested that the system obeys Eley-Rideal mechanism, in which half of the molecules are strongly adsorbed on the active sites, whereas the other part is interacting from the gaseous phase.

To exclude the influence of ethanol readsorption on the acetaldehyde isotope front we have studied the acetaldehyde response during the CH₃CHO-¹³C₂/He/Ar to CH₃CHO/He switch. The results of two different switches, i) acetaldehyde to acetaldehyde-¹³C₂ and ii) labeled ethanol-¹³C₁ to unlabeled ethanol are compared in **Fig. 6**, where acetaldehyde-¹³C₂ response belongs to first switch and the latters were obtained in EtOH-¹³C₁/He/Ar to EtOH/He switch. It is clearly seen that the response of unlabeled butadiene accurately follows the response of ethanol in the EtOH-¹³C₁/He/Ar to EtOH/He switch, while the total response of the single and double-labeled butadiene follows the response of acetaldehyde in acetaldehyde-¹³C₂ to the unlabeled acetaldehyde switch.

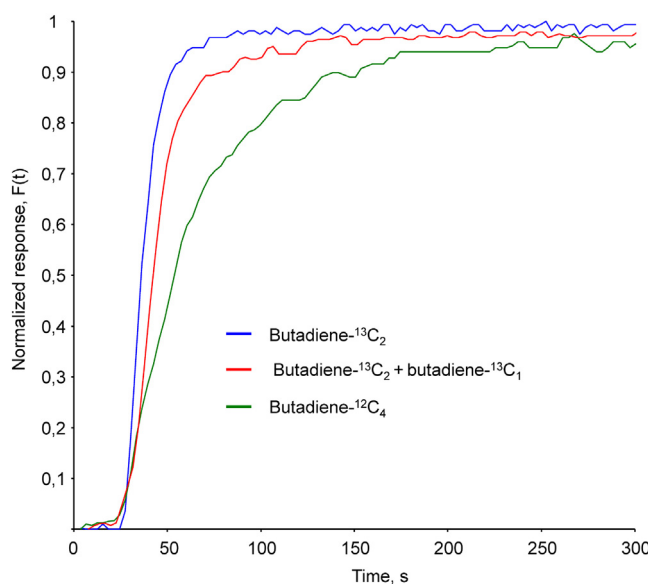


Fig. 5. Normalized isotopic transient response curves of butadiene- $^{12}\text{C}_4$ following the switch from labeled ethanol- $^{13}\text{C}_1$ to unlabeled ethanol compared with butadiene- $^{13}\text{C}_2$ and butadiene- $^{13}\text{C}_1$ responses following the switch from unlabeled ethanol to ethanol- $^{13}\text{C}_1$. Conditions are the following: total flow of $35 \text{ cm}^3 \text{ min}^{-1}$ at 600 K over $\text{Ag}/\text{ZrO}_2/\text{SiO}_2$ catalyst.

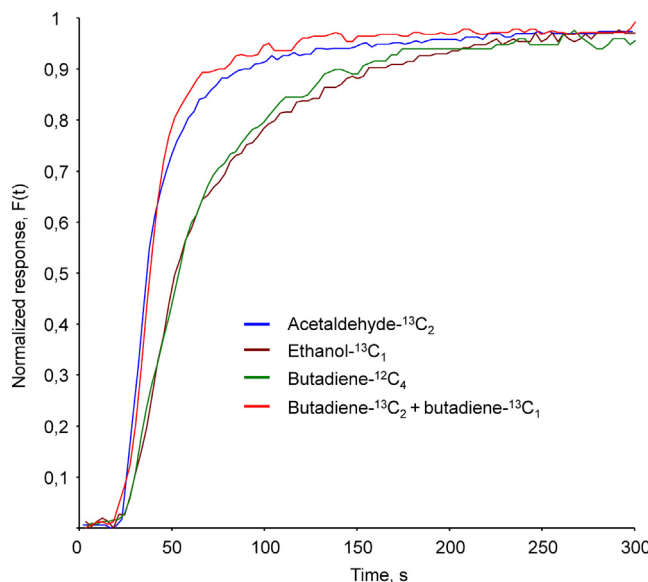


Fig. 6. Comparison of normalized isotopic transient response curves following the switch from unlabeled acetaldehyde to acetaldehyde- $^{13}\text{C}_2$ acetaldehyde. Conditions are the following: total flow of $35 \text{ cm}^3 \text{ min}^{-1}$ at 600 K over $\text{Ag}/\text{ZrO}_2/\text{SiO}_2$ catalyst.

3.4. Label tracing experiments

Label tracing experiments were carried out with specifically labeled deuterated ethanol isotopomers. The information on the label distribution in the products was used to verify the mechanisms of different reaction steps.

3.5. Conversion of $\text{CH}_3\text{CH}_2\text{OH}$

As mentioned in 3.1, the conversion of unlabeled ethanol over the $\text{Ag}/\text{ZrO}_2/\text{SiO}_2$ catalyst leads to the formation of two main products – acetaldehyde and butadiene, with the overall selectivity of 75%. The same selectivity was also observed for all fed isotopomers

of ethanol. It was thus assumed that the formation of by-products will not impact the mechanism analysis significantly.

Mass spectra of acetaldehyde and butadiene obtained by GC-MS of CDCl_3 solutions of the reaction mixture are shown in Fig. 7. Fragmentation of acetaldehyde leads to the appearance of the signals with 15 (CH_3^+ ion), 29 (CHO^+ ion) and 44 m/z (molecular ion CH_3CHO^+). Intensive signals in the range of 41–43 m/z can be attributed to the fragmentation of CH_3CHO^+ ion with subsequent loss of one, two and three protons of methyl group, respectively.

Butadiene mass spectrum shows the presence of signals with mass numbers of 27 ($\text{CH}_2=\text{CH}^+$), 39 ($\text{CH}_2=\text{C}=\text{CH}^+$ ion) and the group of signals in the range of 49–54 with intensive molecular ion signal at 54 m/z.

^1H NMR spectrum of the reaction mixture in CDCl_3 solvent is shown in Fig. 8. Multiplet signals with $\delta = 1.2$ and 3.7 ppm correspond to protons in the CH_3 - and CH_2 - groups of ethanol, whereas signals at 2.3 and 9.8 ppm could be attributed to the CH_3 - and CH -groups of acetaldehyde, respectively. The spectrum region in the range within 5.5–7 ppm shows the ^1H NMR signals of butadiene. Protons of $\text{CH}_2=\text{}$ groups give four signals at 5.10, 5.12, 5.21 and 5.24 ppm, showing the fine structure due to the spin-spin interaction with $-\text{CH}=$ and magnetic splitting. Multiplet signal at 6.35 ppm arises from $-\text{CH}=$ groups interaction with terminal $\text{CH}_2=$ and internal $-\text{CH}=$ groups.

These results are in line with the spectroscopic databases and literature data and will be used for the analysis of isotopomer distribution in the experiments with deuterated ethanol.

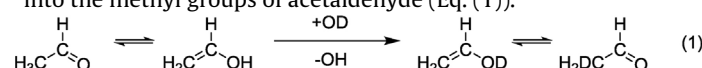
3.6. Conversion of $\text{CD}_3\text{CD}_2\text{OD}$

MS spectra of acetaldehyde and butadiene formed from $\text{CD}_3\text{CD}_2\text{OD}$ are shown in Fig. 9. Acetaldehyde spectrum clearly shows three dominant lines at 18, 30 and 48 m/z, corresponding to the CD_3^+ , CDO^+ , and CD_3CDO^+ ions. Low intensity of the lines with odd m/z values points to the absence of protons in the structure and confirms that the main product observed is CD_3CDO acetaldehyde.

MS spectrum of butadiene reveals the presence of the main signals at 30, 42 and 60 m/z, with low intensity signals with odd m/z, as it was determined for acetaldehyde. Comparison of this spectrum with the spectrum of Fig. 7 points that the product is fully deuterated butadiene. ^1H NMR spectra confirms this suggestion, with no signals of protons typical for ethanol, acetaldehyde or butadiene observed (Fig. 8).

3.7. Reaction with $\text{CH}_3\text{CH}_2\text{OD}$

^1H NMR spectrum of the products obtained from $\text{CH}_3\text{CH}_2\text{OD}$ (Fig. 8c) is similar to those obtained for unlabeled ethanol and do not provide any information on the deuterium tracing during the reaction (Fig. 8). On the contrary, the GC-MS data reveals significant difference between the acetaldehyde and butadiene spectra (Figs. 7, 10). First of all, an intensive signal is observed at 16 (CH_2D^+). Besides, the appearance of the signals at 44, 45 and 46 m/z points to the formation of three acetaldehyde isotopomers: CH_3CHO , CH_2DCHO , and CD_2HCHO with different fractions. Such observation could be explained by a rapid H-D exchange of $\text{CH}_3\text{CH}_2\text{OD}$ with the silanol groups of the support or Zr-OH groups of zirconia followed by H-D exchange of $-\text{OD}$ with acetaldehyde during keto-enol transformation of acetaldehyde, which leads to label transfer into the methyl groups of acetaldehyde (Eq. (1)).



The comparison of the spectral fragments around 29 m/z for $\text{CH}_3\text{CH}_2\text{OD}$ with unlabeled ethanol indicates that deuterium atoms are not involved in $-\text{CH}=\text{O}$ group since no 30 m/z peaks observed,

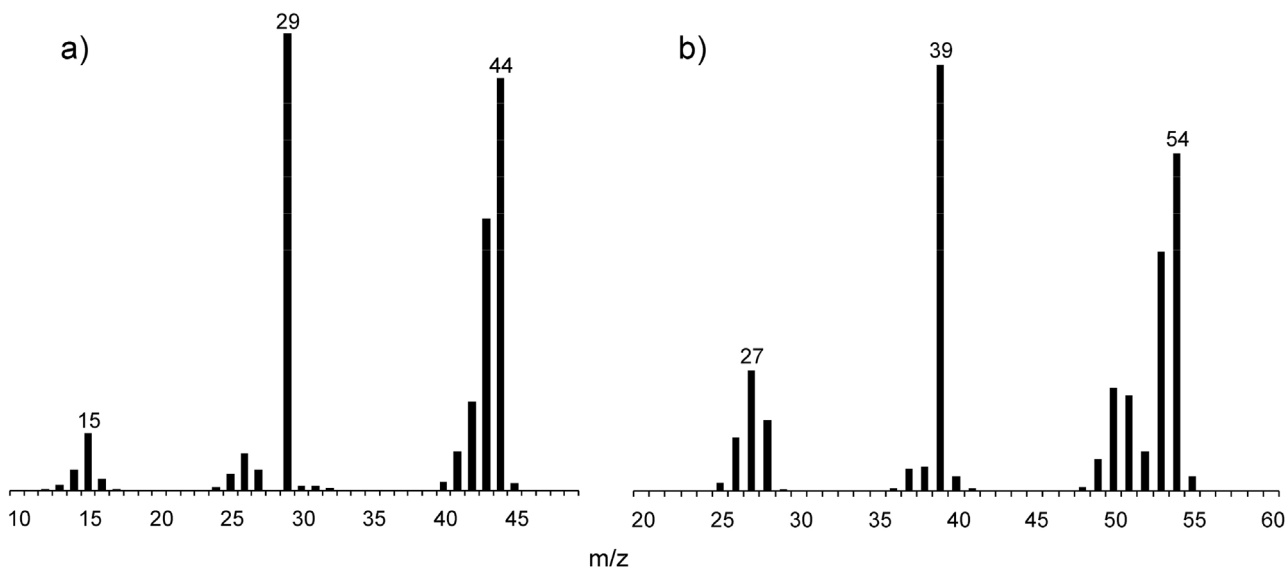


Fig. 7. Mass spectra of acetaldehyde (a) and butadiene (b) formed from $\text{CH}_3\text{CH}_2\text{OH}$ ethanol over $\text{Ag}/\text{ZrO}_2/\text{SiO}_2$ catalyst at 600 K.

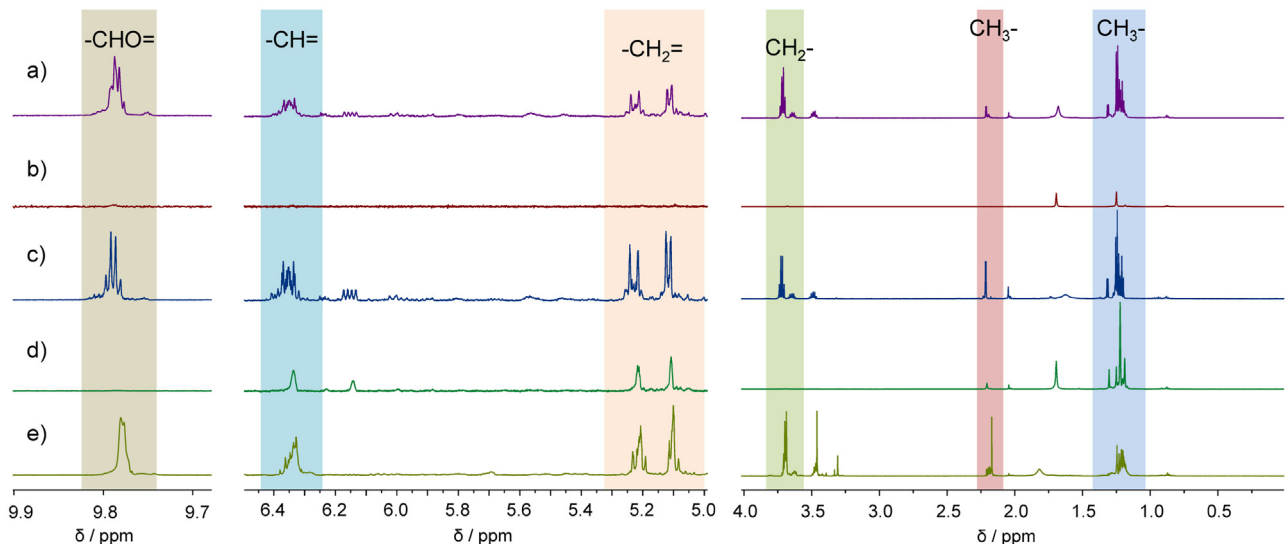


Fig. 8. ^1H NMR spectra of the reaction products formed from a) $\text{CH}_3\text{CH}_2\text{OH}$; b) $\text{CD}_3\text{CD}_2\text{OD}$; c) $\text{CH}_3\text{CH}_2\text{OD}$; d) $\text{CH}_3\text{CD}_2\text{OH}$ and e) $\text{CD}_3\text{CH}_2\text{OH}$.

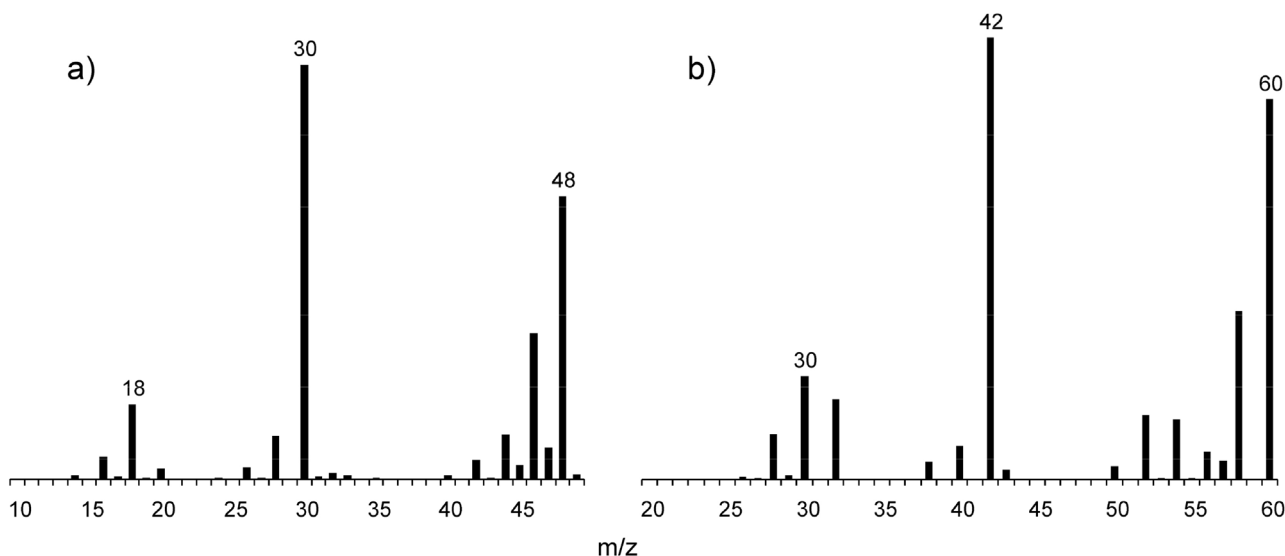


Fig. 9. Mass spectra of acetaldehyde (a) and butadiene (b) formed from $\text{CD}_3\text{CD}_2\text{OD}$ ethanol over $\text{Ag}/\text{ZrO}_2/\text{SiO}_2$ catalyst at 600 K.

Table 4

Distribution of butadiene isotopomers in the reaction of ethanol transformation over Ag/ZrO₂/SiO₂ catalyst (600 K, WHSV = 0.3 h⁻¹, TOS = 30 min).

Reagent	Butadiene isotopomers molar fractions, %						
	C ₄ H ₆	C ₄ H ₅ D	C ₄ H ₄ D ₂	C ₄ H ₃ D ₃	C ₄ H ₂ D ₄	C ₄ HD ₅	C ₄ D ₆
CH ₃ CH ₂ OH	100	0	0	0	0	0	0
CD ₃ CD ₂ OD	0	0	0	0	0	0	100
CH ₃ CH ₂ OD	50	41	9	0	0	0	0
CH ₃ CD ₂ OH	0	0	0	100	0	0	0
CD ₃ CH ₂ OH	—	—	—	—	—	—	—

which strongly supports the keto-enol mechanism of H-D exchange for acetaldehyde. Accordingly, the protons in CHO position of acetaldehyde can not be exchanged with OH or CH₃ groups hydrogen atoms.

Calculation of molar fractions of acetaldehyde isotopomers formed from ethanol using OLS optimization gives the values listed in Table 3, which shows that CH₃CH₂OD dehydrogenation leads to a nearly equimolar mixture of CH₃CHO and CH₂DCHO acetaldehyde isotopomers.

MS spectrum of butadiene formed from CH₃CH₂OD is shown in Fig. 10b. The presence of the molecular ions with 54 and 55 m/z suggests that the significant fraction of butadiene has one deuterium atom in the structure. The small line at 56 m/z indicates the presence of butadiene-D₂ in the reaction mixture. The direct analysis of the isotopomers distribution is complicated because of the absence of the database MS spectra for each isotopomer of butadiene. Notwithstanding, the form of MS spectrum points to a significant amount of unlabeled butadiene in the mixture. To simplify the interpretation the spectrum of butadiene-H₆ (Fig. 7b) was subtracted from the spectrum of the mixture (Fig. 10b). The result is shown in Fig. S2.

The subtracted spectrum reveals the presence of the main lines at 28, 39, 40 and 55 m/z, which could be attributed to the butadiene with one deuterium atom in the structure (Fig. S2). Unfortunately, it is not possible to evaluate the position of the deuterium due to the similar schemes of the fragmentation of the isotopomers with deuterium in CHD= and -CD=groups. The relative amounts of C₄H₆, C₄H₅D, and C₄H₄D₂ isotopomers obtained by the OLS optimization are presented in Table 4.

Summarizing MS and ¹H NMR data, it can be concluded that the transformation of CH₃CH₂OD leads to predominant formation of two isotopomers: C₄H₆ and C₄H₅D, and the latter may contain deuterium atom both in the CHD= or -CD=groups. Besides, a small amount of C₄H₄D₂ isotopomer is detected.

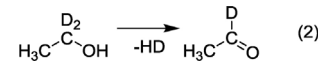
Taking into account that ethanol dehydrogenation and keto-enol isomerization result predominantly in two isotopomers of acetaldehyde, four transformation routes with equal probabilities of 1/4 can be considered (Scheme S1). By summarizing and multiplying of the probabilities, the following probabilities of four isotopomers formation were calculated: P(C₄H₆) = 20/9; P(C₄H₅D₁) = 10/9 + 4/9 = 14/9 and P(C₄H₄D₂) = 2/9. The comparison of the calculated and experimental data (Table 4) shows good correlation and suggests that the mechanism of aldol condensation involves the enolization step.

3.8. Conversion of CH₃CD₂OH

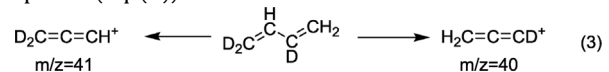
Conversion of CH₃CD₂OH over Ag/ZrO₂/SiO₂ catalyst exhibits interesting deuterium distribution for acetaldehyde and butadiene.

¹H NMR spectrum shows significant changes with respect to unlabeled ethanol and CH₃CH₂OD (Fig. 8). Signals at 3.7 ppm attributed to CH₂- groups of ethanol vanish from the spectra, as does the signal at 9.8 ppm attributed to the -CH= protons of acetaldehyde. The observation of the singlet signal at 2.3 ppm typical for CH₃-groups of acetaldehyde confirms the formation of -CD= labeled acetaldehyde. Proton signals of butadiene (Fig. 8) also point to the deuterium substitution of H atoms. Two singlet signals at 5.11 and 5.21 ppm instead of two doublet signals observed for C₄H₆ molecule point to the loss of magnetic inequivalence of the protons in the methylene groups and could be accompanied by full substitution of one terminal CH₂= with deuterium. Furthermore, broad singlet at 6.34 clearly points to the presence of only one H atom in -CH= position. Thus, NMR data suggests that CH₃CD₂OH ethanol converts predominantly into C₄H₃D₃ products, with two deuterium atoms included in the terminal CD₂= group and the third one substituting a proton in the -CD= fragment.

Further analysis on the isotopomer structure of the products was based on GC-MS data. The MS spectrum of acetaldehyde formed from CH₃CD₂OH confirms the suggestions made by the NMR analysis (Fig. 11a). The observation of molecular ion with 45 m/z points to the formation of D₁ substituted acetaldehyde, and intensive signal at 30 m/z indicates the position of deuterium in CDO⁺ ion (Eq. (2)).



The MS spectrum of butadiene formed from CH₃CD₂OH ethanol reveals the presence of molecular ion at 57 m/z, which confirms the formation of C₄H₃D₃ butadiene (Fig. 11b). The presence of two intensive MS signals at 40 and 41 m/z with equal probability of the CH₂= group abstraction, gives the clear structure of butadiene isotopomer (Eq. (3)).



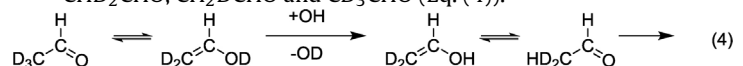
This structure is in line with NMR data discussed above. The only formation of CD₂CHCDCH₂ isotopomer provides unique information on the mechanism MPVO step, which will be discussed in 4.3.

3.9. Reaction with CD₃CH₂OH

Fig. 12a shows the presence of different molecular ions for acetaldehyde from 44 to 47 m/z, which points on the formation of the once, twice and three times D-substituted isotopomers of acetaldehyde. The presence of different ions within the range of 15–18 m/z confirms this suggestion. Since only one line at 29 m/z is observed, it could be suggested that deuterium substitutions occurs only in methyl group of acetaldehyde.

To calculate the fractions of each isotopomer in the final mixture, the theoretical MS spectra for CHD₂CHO, CH₂DCHO and CD₃CHO were modelled under the assumption that isotopical substitution does not effect the relative intensities of the molecular ions and other fragments in MS spectrum in comparison with CH₃CHO molecule. The values obtained after OLS optimization are summarized in Table 4.

The observations made for D-tracing during the transformation of CD₃CH₂OH are similar to those found for CH₃CH₂OD reagent (Eq. (1)). The exchange of surface OH groups with the deuterated hydroxyl groups of enol leads to the deuterated acetaldehyde CHD₂CHO, CH₂DCHO and CD₃CHO (Eq. (4)).



The analysis of the transformation routes of these isotopomers mixture in the butadiene synthesis seems to be rather complicated.

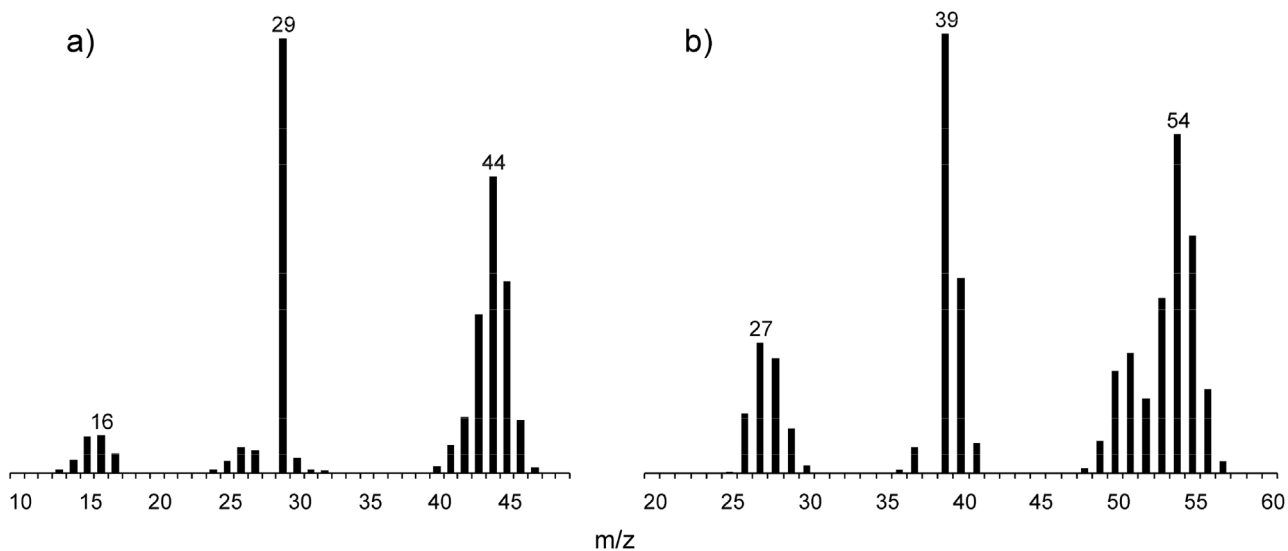


Fig. 10. Mass spectra of acetaldehyde (a) and butadiene (b) formed from $\text{CH}_3\text{CH}_2\text{OD}$ ethanol over $\text{Ag}/\text{ZrO}_2/\text{SiO}_2$ catalyst at 600 K.

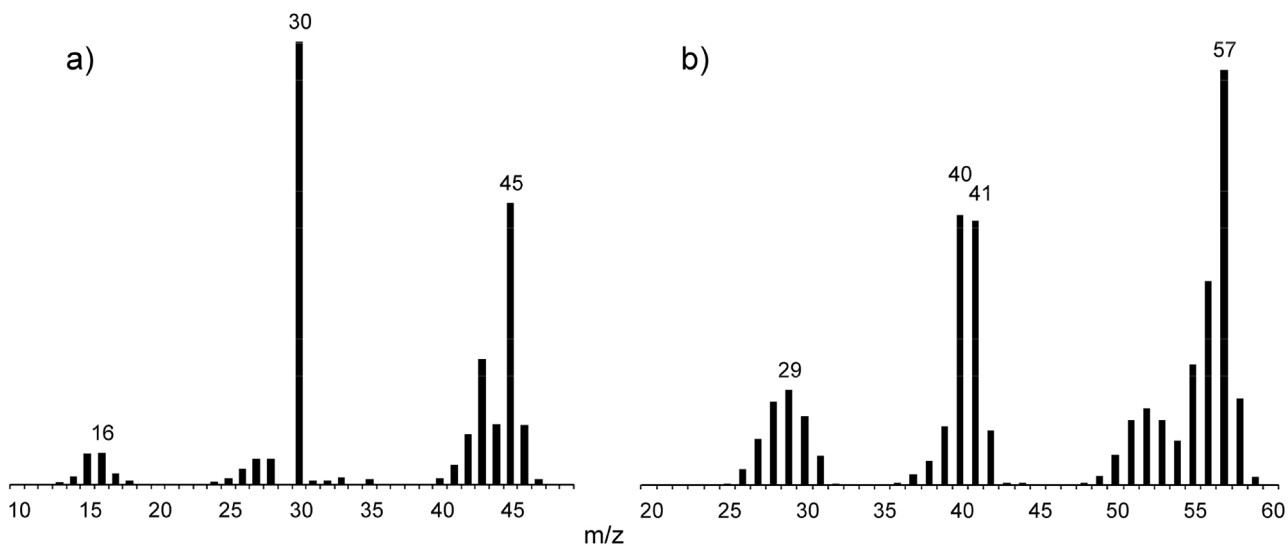


Fig. 11. Mass spectra of acetaldehyde (a) and butadiene (b) formed from $\text{CH}_3\text{CD}_2\text{OH}$ ethanol over $\text{Ag}/\text{ZrO}_2/\text{SiO}_2$ catalyst at 600 K.

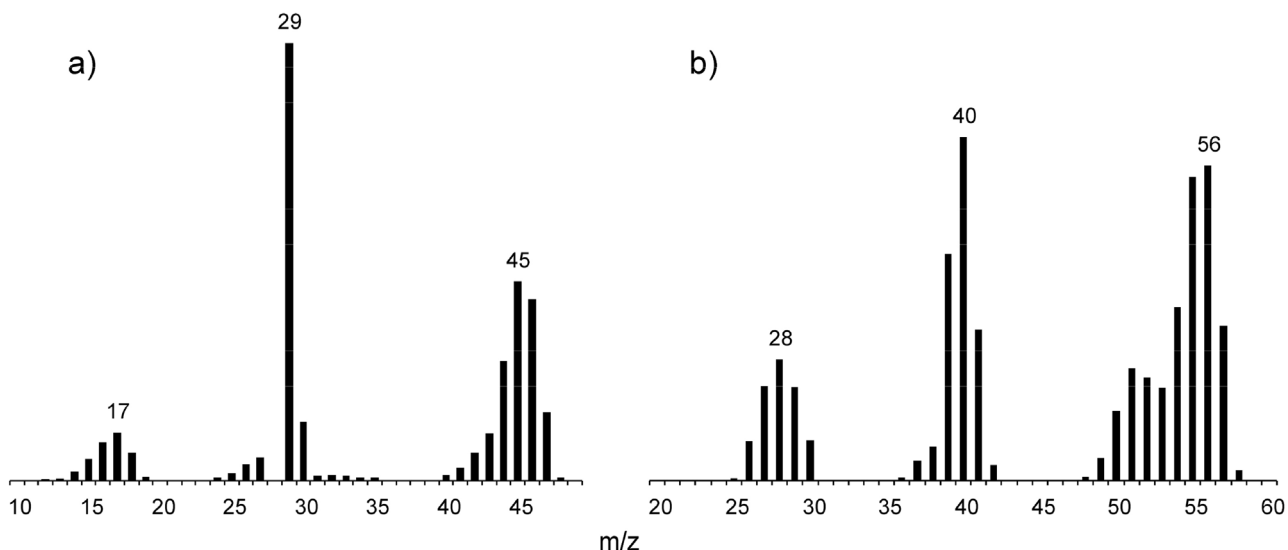


Fig. 12. Mass spectra of acetaldehyde (a) and butadiene (b) formed from $\text{CD}_3\text{CH}_2\text{OH}$ ethanol over $\text{Ag}/\text{ZrO}_2/\text{SiO}_2$ catalyst at 600 K.

Table 3

Distribution of acetaldehyde isotopomers in the reaction of ethanol transformation over Ag/ZrO₂/SiO₂ catalyst (600 K, WHSV = 0.3 h⁻¹, TOS = 30 min).

Reagent	Acetaldehyde isotopomers molar fractions, %					
	CH ₃ CHO	CH ₃ CDO	CD ₃ CHO	CH ₂ DCHO	CHD ₂ CHO	CD ₃ CDO
CH ₃ CH ₂ OH	100	0	0	0	0	0
CD ₃ CD ₂ OD	0	0	0	0	0	100
CH ₃ CH ₂ OD	50	0	0	41	9	0
CH ₃ CD ₂ OH	0	100	0	0	0	0
CD ₃ CH ₂ OH	11	0	23	27	39	0

The mass spectrum of the mixture reveals the presence of the lines typical for C₄H₆, C₄H₅D, C₄H₄D₂, and C₄H₃D₃ isotopomers; however, their structure can not be unambiguously determined. ¹H NMR spectrum of the products mixture formed from CD₃CH₂OH confirms the GC-MS data. Butadiene ¹H spectrum consists of several signals which belong to different compounds (Fig. 8).

4. Discussion

The analysis of the results of kinetic, SSITKA and label tracing studies points that each technique provides valuable information for the understanding of the mechanism of the key reaction steps. The comparison of these results and their joint analysis allows unraveling the mechanism of each reaction step and reconstructing the overall reaction mechanism.

4.1. Rate-determining step

One of the central questions in the mechanistic studies of the multistep catalytic reactions, such as ethanol conversion into butadiene, is connected with the determination of the rate-limiting step of the overall reaction. Previous studies have demonstrated that over the mixed oxide catalysts without metal promoter or with low metal promoter loadings the rate-limiting step is ethanol dehydrogenation [8–12,14,16,17,19,20,23,26,27]. In the case of bifunctional metal promoted oxide catalysts with balanced composition ethanol dehydrogenation step does not significantly affect the butadiene synthesis rate and acetaldehyde condensation becomes rate-determining [8–10,16,29,44,45].

For the present study we have selected Ag/ZrO₂/SiO₂ catalyst with good balance of active components [8]. The kinetic study performed previously [8] suggested that among the five reaction steps, which constitute the target reaction pathway (Scheme 1), three steps involving i) ethanol dehydrogenation, ii) acetaldehyde aldol condensation, and iii) MPVO reduction of crotonaldehyde can be considered as the key reaction steps leading to butadiene. Dehydration of 3-hydroxybutanal and crotyl alcohol was shown to proceed easily, even on the weak acid sites of silica support. The aldol condensation was suggested to be the rate-limiting step over this catalyst.

The results obtained in the present study confirm this conclusion. Thus, the kinetic measurements show that butadiene formation rate is strongly controlled by the acetaldehyde partial pressure exhibiting non-linear dependence (Figs. 2 a, 3). Addition of small amounts of crotonaldehyde significantly increases the rate of the butadiene formation (Fig. 3c). The KIE observed for the CD₃CH₂OH deuterated ethanol (Table 1) confirms the participation of the methyl group protons of the formed acetaldehyde with significant impact to the overall reaction rate. Furthermore, butadiene/acetaldehyde formation rate ratios for CD₃CD₂OD and CD₃CH₂OH demonstrate similar values (Table 1), indicating that the C-D cleavage in the CD₃ group governs the rate of the butadiene formation.

Although aldol condensation was found to be rate-determining over Ag/ZrO₂/SiO₂ catalyst, dehydrogenation and MPVO reduction

steps were also considered in this study as the key reaction steps playing an important role in the overall reaction mechanism. Therefore, further investigations were focused at the detailed analysis of these steps based on kinetic, SSITKA, and label tracing studies.

4.2. Ethanol dehydrogenation step

The investigation of the ethanol adsorption by the SSITKA approach (Fig. 4) points that normalized response of ethanol decays very slowly. In addition, zero space time correction shows significant readsorption effect (Table 2). Such behavior suggests strong adsorption of ethanol molecules, most probably, over silanol groups of the catalyst.

The analysis of the kinetic isotope effects observed for acetaldehyde formation points to the highest effects in the case of the CH₃CH₂OD and CH₃CD₂OH labeled substrates (Table 1). Similar acetaldehyde formation rates for these isotopomers suggest that the cleavage of the α-C–H bond and the proton abstraction from OH group proceed simultaneously, which is an argument in favor of the concerted mechanism suggested previously for the ethanol dehydrogenation over Ag/SiO₂ [48]. The higher overall KIE value in the case of CH₃CD₂OH can be explained by the involvement of CD₂ in further reaction steps. Fully deuterated ethanol shows the highest KIE and the lowest acetaldehyde formation rate, which is also in line with the concerted mechanism of dehydrogenation [48]. For the CD₃CH₂OH isotopomer only slight difference in acetaldehyde formation rate in comparison with unlabeled ethanol is observed, which confirms that the CD₃-groups are not involved in the dehydrogenation of ethanol.

Similar mechanistic features of ethanol dehydrogenation observed over Ag/SiO₂ and Ag/ZrO₂/SiO₂ suggest that this reaction step takes place over the same active sites, namely, bifunctional sites containing silanol groups and Ag particles. The interaction of ethanol with surface silanol groups of Ag/ZrO₂/SiO₂ is confirmed by the rapid H–D exchange at the early steps of the reaction. Thus, the analysis of deuterium label distribution in acetaldehyde (Table 3) formed from the specifically labeled ethanol molecules points to a significant contribution of the H–D exchange in the methyl group of acetaldehyde. In particular, the conversion of CH₃CH₂OD gives 50% of CH₃CHO, 41% of CH₂DCHO and 9% of CHD₂CHO. Similarly, the conversion of CD₃CH₂OH results in 39% of CHD₂CHO, 27% CH₂DCHO and 11% of CH₃CHO. These results can be accounted for by the rapid H–D exchange between the hydroxyl group of ethanol and surface silanol groups, which is accompanied by further H–D exchange between silanol groups and methyl groups of acetaldehyde due to keto-enol tautomerism in acetaldehyde (Eqs. 1 and 4). Observed difference in the label distribution for acetaldehyde formed from CH₃CH₂OD and CD₃CH₂OH corresponds to the different fraction of D-atoms able to undergo H–D exchange. Thus, the fraction of labile protons in CH₃CH₂OD is 0.25 while for CD₃CH₂OH it accounts for 0.75.

According to Ref. 48, the mechanistic pathway for ethanol dehydrogenation over the Ag/SiO₂ sites involves the formation of H-bonded complex with Si–OH groups followed by the concerted C–H cleavage on silver site and proton abstraction on silica site

resulting in the formation of hydrogen adsorbed on silver site and acetaldehyde adsorbed on silica (**Scheme 2**). The last step should be the desorption of H₂ and acetaldehyde leading to the regeneration of the active site.

Comparison of the readsorption corrected values of residence times measured by SSITKA for ethanol and acetaldehyde shows that they are similar (**Table 2**). However, the acetaldehyde response during acetaldehyde-¹³C₂ to unlabeled acetaldehyde switch (**Fig. 6**) is faster than the ethanol response during ethanol-¹³C₁ to unlabeled ethanol switch indicating weaker adsorption of acetaldehyde over the catalyst. It can be thus concluded that acetaldehyde molecules formed are easily replaced by ethanol over the Ag/SiO₂ active sites.

Summarizing the results discussed above, we can suggest that ethanol dehydrogenation reaction represents a separate catalytic cycle over Ag-containing sites coupled with silanol groups (**Cycle I** in **Scheme 2**). The reaction starts with ethanol adsorption on silica to yield a hydrogen-bonded surface complex. The next step is a concerted α -C—H bond cleavage on a Ag site and a proton abstraction on a silica site. The final step of the reaction includes desorption of hydrogen and acetaldehyde into gas phase, which regenerates the active sites.

4.3. Acetaldehyde aldol condensation step

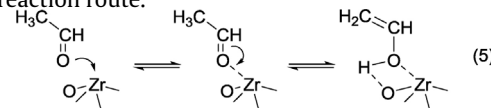
Condensation of acetaldehyde is the next step of acetaldehyde transformation. It involves the C—C coupling giving the C₄ precursors of butadiene. The reaction can proceed over both basic [11,12,14,16–18,23,26,27,29,49] and acidic [8–10,13,15,22,28,31,49] sites leading to 3-hydroxybutanal, which further dehydrates into crotonaldehyde. This step is considered to be the most important in the overall process. The insight into the active sites responsible for this reaction step and the information on its mechanism are crucial for the design of efficient catalysts for ethanol conversion into butadiene. [8–11,15,16,23].

It has been previously demonstrated that Lewis acid sites are responsible for aldol condensation over solid acid catalysts [10,49,50]; however, different mechanistic pathways were proposed to account for acetaldehyde interaction with Lewis sites. In particular, stepwise mechanistic pathways involving intermediate enol formation [51–53] and concerted mechanisms [50] were suggested. To verify which of these mechanisms is operating under the conditions of butadiene synthesis, D-tracing experiments were performed. The results on H-D exchange in acetaldehyde obtained during the transformation of specifically labeled ethanol molecules, namely, CD₃CH₂OH and CH₃CH₂OD (**Table 3**, Eqs. (1) and (4)) point to the intermediate formation of enol species and suggest that stepwise mechanism is operating under the reaction conditions employed in this study.

The kinetic isotope effect for butadiene formation observed for the CD₃CH₂OH labeled ethanol supports this suggestion (**Table 1**). The rate of butadiene formation from CD₃CH₂OH is significantly lower with respect to unlabeled ethanol, and butadiene to acetaldehyde formation rate ratio is close to those observed for fully deuterated ethanol. Thus, the activation of acetaldehyde molecule implies the formation of the enol form (**Eq. (5)**). Stabilization of enol formed can proceed via two pathways: 1) complete abstraction of α -proton of acetaldehyde molecule with formation of CH₂[–] anion [54,55], and 2) bonding of protons of OH group of enol to neighboring oxygen atom which acts as weak Brønsted base [50,56]. First pathway is generally accepted for the catalysts, possessing pronounced basic properties, such as magnesia, hydroxyapatites and calcium phosphate. The presence of strong basic sites (O^{2–} sites and basic OH groups) enables the proton abstraction and stabilizes the enol-anion formed. Therefore, for basic catalysts no KIE was observed for fully deuterated acetaldehyde [54]. Likely,

presence of strong basic sites makes the proton abstraction step very fast hence explaining absence of KIE for deuterium labeled acetaldehyde.

On contrary, for Lewis acid catalysts both mechanisms are valid. For SnBEA [50,51–53] and HfBEA [51,53] catalysts the formation of enol stabilized over metal sites and corresponding silanol group has been reported pointing to the complete α -H transfer to the O atoms. In the case of TiBEA and ZrBEA [50] the formation of silanol groups has not been observed by infrared spectroscopy indicating the possible stabilization of enol via coordination to weak basic oxygen atoms near the metal sites. FTIR experiments carried out for ZrO₂/SiO₂ catalyst (**Fig. S8**) have not shown the formation of any OH groups during the acetaldehyde adsorption. Therefore, the α -H transfer to oxygen atoms seems to be unlikely in the case of ZrO₂-based catalysts. Assuming the absence of strong basic sites on silica supported catalysts [49] and considerable kinetic isotope effect observed for CD₃CH₂OH labeled ethanol conversion (**Table 1**), acetaldehyde enolization over Ag/ZrO₂/SiO₂ mostly proceeds via second reaction route.



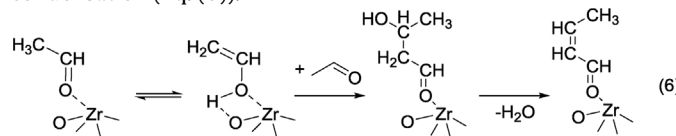
The interaction of activated acetaldehyde molecule adsorbed over the Zr Lewis acid site with another CH₃CHO molecule can proceed through two different mechanisms: 1) adsorption of the second acetaldehyde molecule on the same Lewis site or neighboring silanol group followed by interaction with enol (Langmuir-Hinshelwood mechanism); or 2) interaction of acetaldehyde molecule with adsorbed enol directly from gaseous phase (Eley-Rideal mechanism).

The discrimination between these mechanisms can be done by the SSITKA approach. Comparing the decay for double labeled butadiene-¹³C₂ with the response of unlabeled butadiene, it can be noticed that double labeled butadiene-¹³C₂ decays significantly faster during the EtOH-¹³C₁/EtOH-¹²C₂ switch (**Fig. 4**). Furthermore, the total response for both ¹³C₂ and ¹³C₁ labeled butadiene (**Fig. 5**) is faster than unlabeled butadiene, which response is similar to acetaldehyde and ethanol (**Fig. 4**). This indicates that one C₂ fragment of butadiene molecule arises from the enol species that are strongly interacting with the surface of the catalyst revealing slow SSITKA normalized response. Whereas the another C₂ fragment shows very fast response after isotope switch and can be attributed to acetaldehyde molecule interacting with surface enol directly from the gas phase.

Conversion of ethanol over Ag/ZrO₂/SiO₂ catalyst does not allow accurate comparison of the decays of acetaldehyde and butadiene due to strong readsorption effect of ethanol, which results in slow decay of acetaldehyde. The study of acetaldehyde response during the acetaldehyde-¹³C₂ to acetaldehyde-¹²C₂ isotope switch in SSITKA experiments exclude the ethanol readsorption effect and can be compared with butadiene response (**Fig. 6**).

It is clearly seen that the response of unlabeled butadiene accurately follows the response of ethanol in the EtOH-¹³C₁/EtOH-¹²C₂ switch, while the total response of single and double-labeled butadiene follows the response of acetaldehyde in the acetaldehyde-¹³C₂ to acetaldehyde-¹²C₂ isotope switch. This data confirms the Eley-Rideal mechanism of the acetaldehyde condensation implying the interaction adsorbed acetaldehyde with acetaldehyde molecules from gaseous phase. 3-Hydroxybutanal formed undergoes an easy dehydration leading to crotonaldehyde. This conclusion is strongly supported by the results of kinetic study (**Fig. 3a**). At low partial pressures of acetaldehyde the butadiene formation rate showed linear trend, while at pressure higher than 0.15 bar it has zero order to acetaldehyde due to the saturation of the surface active sites.

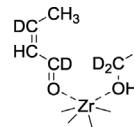
The obtained results point to the following mechanism of aldol condensation (Eq. (6)).



The reaction starts from the adsorption of the acetaldehyde molecule over the Zr Lewis acid site of the catalyst. At the next step, the acetaldehyde undergoes the enolization forming the enol adsorbed over Zr site and neighboring O atom which can interact with another acetaldehyde molecule directly from the gaseous phase according to Eley-Rideal mechanism. Acetaldol formed dehydrates easily yielding crotonaldehyde adsorbed over Zr site.

4.4. Crotonaldehyde MPVO reduction step

Further transformation of crotonaldehyde involves the MPVO reduction with ethanol giving crotyl alcohol and, subsequently,

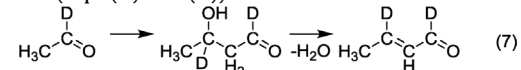


butadiene (**Scheme 1**). This reaction was also shown to proceed over the Zr Lewis sites in the case of various Zr-containing catalysts [57]. The mechanism of Lewis acid catalyzed MPVO reduction was first proposed for homogeneous catalysts [58] and involved the formation of a six-member ring transition complex followed by an H-shift from the alcohol molecule to carbonyl group of aldehyde or ketone. In the case of heterogeneous catalysis, DFT calculations suggested that the similar mechanism is valid for the Lewis acid catalysts implying the adsorption of both aldehyde and alcohol molecule over one site [59].

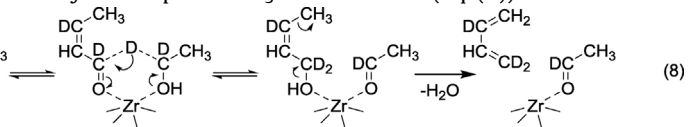
The adsorption of crotonaldehyde and ethanol molecules over one active site can be verified from the kinetic experiments shown in **Fig. 3c**. The butadiene formation rate curve for fixed crotonaldehyde partial pressures and varied ethanol pressures exhibits maxima at 0.1–0.2 bar. The decrease of the butadiene forma-

tion rate at the ethanol pressures higher than 0.2 bar is due to the competitive adsorption of ethanol over the sites occupied by crotonaldehyde and its transformation products. The shape of this curve is typical for bimolecular Langmuir-Hinshelwood mechanism, which implies the interaction of crotonaldehyde and ethanol molecules adsorbed over one active site. Thus, it can be suggested that MPVO reduction step proceeds via bimolecular Langmuir-Hinshelwood mechanism, requiring the adsorption of crotonaldehyde and ethanol molecules over the same Zr Lewis site.

To verify the mechanism of the crotonaldehyde reduction with ethanol D-tracing experiments for $\text{CH}_3\text{CD}_2\text{OH}$ labeled ethanol were performed over the $\text{Ag}/\text{ZrO}_2/\text{SiO}_2$ catalyst. The formation of exclusively CH_3CDO acetaldehyde (**Table 3**) and $\text{CD}_2=\text{CH}-\text{CD}-\text{CH}_2$ butadiene (**Table 4**) isotopomers confirms the following reaction mechanism (Eqs. (7) and (8)).



Condensation of CH_3CDO acetaldehyde leads to the only crotonaldehyde isotopomer $\text{CH}_3-\text{CD}=\text{CHCD}=O$ (Eq. (7))

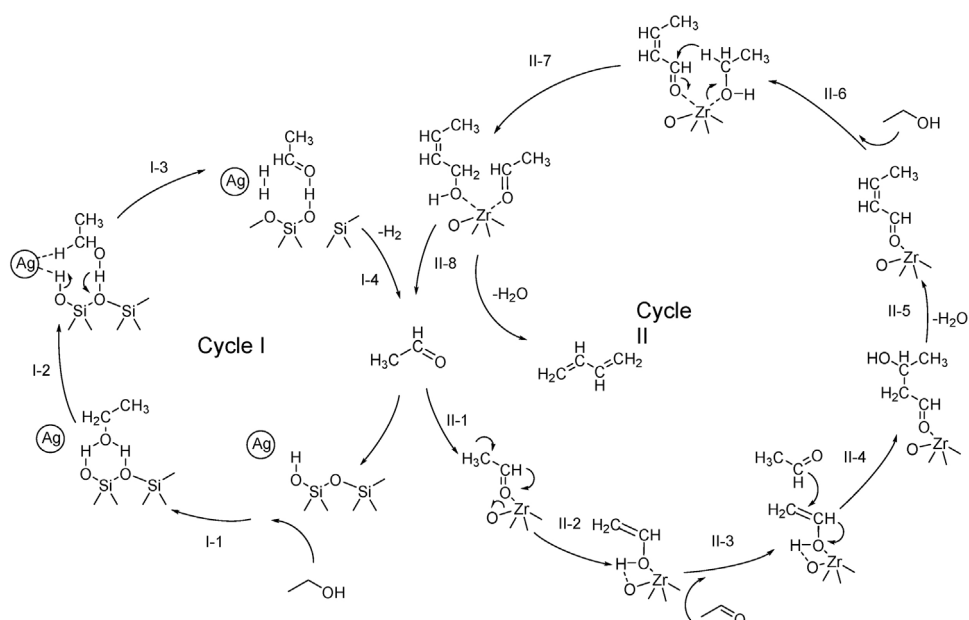


This isotopomer can be selectively converted into $\text{CD}_2=\text{CH}-\text{CD}-\text{CH}_2$ butadiene via the only mechanistic pathway, considering single-site adsorption of crotonaldehyde and ethanol and including the formation of the six-member ring transition complex followed by D-shift of ethanol CD_2 group deuterium atoms to the C=O group of crotonaldehyde (Eq. (8)).

Summarizing the results, steps 2–5 of the overall reaction mechanism (**Scheme 1**) are shown to proceed over the same active sites and therefore can be rationalized in one catalytic cycle operating over these sites.

4.5. Overall reaction mechanism of ethanol transformation into butadiene

The analysis of the mechanisms proposed for different reaction steps allows to rationalize the overall reaction mechanism in



Scheme 2. Proposed mechanism of butadiene formation from ethanol over bifunctional Ag-promoted zirconia catalysts.

two catalytic cycles, including ethanol dehydrogenation over the Ag/Si-OH sites and acetaldehyde condensation followed by crotonaldehyde reduction with ethanol over Zr Lewis sites as shown in Scheme 2.

The reaction starts with the ethanol adsorption over silanol groups leading to H-bonded ethanol complex (Step I-1). Following transformations involve concerted abstraction of molecular hydrogen from the CH₂ group of ethanol and proton transfer from the H-bonded ethanol complex (Steps I-2 and I-3) leading to acetaldehyde, which desorbs into the gas phase (Step I-4). These suggestions are strongly supported by SSITKA and KIE results as well as our recent work on ethanol dehydrogenation [48].

All the following reaction steps take place over Zr Lewis sites and represent the second reaction cycle. This catalytic cycle involves: II-1) the adsorption of acetaldehyde over Zr Lewis acid sites; II-2) its activation via enolization with stabilization on zirconium-oxygen pair site; II-3,4) aldol condensation according to Eley-Rideal mechanism, implying the second acetaldehyde molecule interacting with activated acetaldehyde from the gaseous phase; II-5) dehydration of 3-hydroxybutanal formed into crotonaldehyde adsorbed over Zr-site; II-6) adsorption of ethanol molecule over the same site; II-7) MPVO reduction of crotonaldehyde via 6-member ring transition state, in which proton of methylene CH₂ groups of ethanol shifts to the carbonyl group of crotonaldehyde leading to crotyl alcohol and acetaldehyde; II-8) dehydration of crotyl alcohol leading to butadiene, which desorbs into gaseous phase and acetaldehyde, liberated for the next catalytic turnover.

The proposed mechanism suggests that for the rational design of the optimal catalyst for the selective synthesis of butadiene from ethanol, the dehydrogenation function provided by metal sites and the acidic function provided by Lewis sites should be carefully balanced in the overall bifunctional catalyst.

5. Conclusions

For the first time, the molecular-level mechanism of butadiene formation from ethanol over silica-supported silver promoted zirconia catalyst was studied using kinetic measurements, SSITKA and deuterium label tracing techniques. It was shown that butadiene synthesis involves two independent catalytic cycles responsible for: 1) ethanol dehydrogenation over Ag/Si-OH sites and 2) acetaldehyde/ethanol transformation into butadiene over Zr Lewis acidic sites.

The first catalytic cycle includes strong adsorption of ethanol over surface silanol groups via H-bonding followed by concerted C–H cleavage of the CH₂ and OH groups of ethanol over bifunctional Ag/Si-OH site. Acetaldehyde and hydrogen are further desorbed into the gaseous phase, liberating the active site for the next catalytic cycle. The proposed mechanism is confirmed by SSITKA measurements of ethanol-¹³C₁/ethanol-¹²C₂ switches, D-tracing experiments for CH₃CH₂OD, KIE analysis of CH₃CH₂OD and CH₃CD₂OH transformations as well as our recent study on ethanol dehydrogenation over Ag/SiO₂ [48].

The second cycle starts with the activation of acetaldehyde over Zr Lewis acid sites via enolization and stabilization over Zr-O pair sites confirmed by D-tracing experiments for CH₃CH₂OD and CD₃CH₂OH and KIE analysis of CD₃CH₂OH transformation. The activated acetaldehyde interacts further with the second acetaldehyde molecule from the gaseous phase according to Eley-Rideal mechanism confirmed by SSITKA measurements of ethanol-¹³C₁/ethanol-¹²C₂ and acetaldehyde-¹³C₂/acetaldehyde-¹²C₂ switches. The formed 3-hydroxybutanal undergoes fast dehydration into crotonaldehyde adsorbed on the Zr site. The next step involves adsorption of ethanol molecule on the same Zr site and MPVO reduction of crotonaldehyde with ethanol via the six-member ring transition state verified by the D-tracing

experiments for CH₃CD₂OH. This step proceeds according to the Langmuir-Hinshelwood model as confirmed by kinetic studies of crotonaldehyde interaction with ethanol. Finally, crotyl alcohol undergoes fast dehydration into the target butadiene and butadiene desorbs into the gaseous phase. The acetaldehyde adsorbed over Zr sites initiates the next catalytic turnover.

Aldol condensation of acetaldehyde is found to be the rate-limiting step of the overall process over silver promoted zirconia based catalyst as confirmed by the kinetic analysis and kinetic isotope effect for specifically deuterated ethanol.

Considering the nature of the active sites involved in each catalytic cycle, we suggest that the provided mechanism is valid for the catalysts based on metal (i.e. Cu, Ag and Au) promoted Lewis acids like Zr and Ta substituted zeolites or supported zirconium and hafnium oxides [8–10,22,28,29,31]. Our further work is focused on the mechanism of this reaction over basic catalysts like MgO and MgO supported on various supports.

The proposed mechanism provides useful information for further design of efficient catalysts of butadiene synthesis from ethanol and for the improvement of the reaction conditions. In particular, the improvement of acidic component will result in the enhancement of its activity in aldol condensation step and ramped pressure can be applied to increase the catalyst activity according to Eley-Readel mechanism of aldol condensation step.

Acknowledgements

The authors thank the Russian Science Foundation for the financial support (Grant no. 14-23-00094).

Appendix A. Supplementary data

Supplementary data associated with this article can be found, in the online version, at <http://dx.doi.org/10.1016/j.apcatb.2017.05.060>.

References

- [1] J.J. Bozell, G.R. Petersen, Green Chem. 12 (2010) 539–554.
- [2] C. Angelici, B.M. Weckhuysen, P. Bruijnincx, ChemSusChem 6 (2013) 1595–1614.
- [3] E.V. Makshina, M. Dusselier, W. Janssens, J. Degrève, P. Jacobs, B. Sels, Chem. Soc. Rev. 43 (2014) 7917–7953.
- [4] A.D. Patel, K. Meesters, H. den Uil, E. de Jong, K. Blok, M.K. Patel, Energy Environ. Sci. 5 (2012) 8430–8444.
- [5] J.A. Posada, A.D. Patel, A. Roes, K. Blok, A.C. Faaij, M.K. Patel, Biores. Technol. 135 (2013) 490–499.
- [6] J. Sun, Y. Wang, ACS Catal. 4 (2014) 1078–1090.
- [7] W.C. White, Chem.-Biol. Interact. 166 (2007) 10–14.
- [8] V.L. Sushkevich, I. Ivanova, V. Ordovsky, E. Taarning, ChemSusChem 9 (2014) 2527–2536.
- [9] V.L. Sushkevich, I.I. Ivanova, E. Taarning, Green Chem. 17 (2015) 2552–2559.
- [10] V.L. Sushkevich, D. Palagin, I.I. Ivanova, ACS Catal. 5 (2015) 4833–4836.
- [11] C. Angelici, M.E.Z. Velthoorn, B.M. Weckhuysen, P.C.A. Bruijnincx, ChemSusChem 7 (2014) 2505–2515.
- [12] E.V. Makshina, W. Janssens, B.F. Sels, P.A. Jacobs, Cat. Today 198 (2012) 228–344.
- [13] M. Jones, C. Keir, C.D. Iulio, R. Robertson, C. Williams, D. Apperley, Catal. Sci. Technol. 1 (2011) 267–272.
- [14] M. Lewandowski, G.S. Babu, M. Vezzoli, M.D. Jones, R.E. Owen, D. Mattia, P. Plucinski, E. Mikolajski, A. Ochenduszko, D.C. Apperley, Catal. Commun. 49 (2014) 25–28.
- [15] H.-T. Chae, T.-W. Kim, Y.-K. Moon, H.-K. Kim, K.-E. Jeong, C.-U. Kim, S.-Y. Jeong, Appl. Catal. B Environ. 150–151 (2014) 596–604.
- [16] W. Janssens, E. Makshina, P. Vanelderen, F. De Clippel, K. Houwhoofd, S. Kerkhofs, J.A. Martens, P.A. Jacobs, B.F. Sels, ChemSusChem 8 (2015) 994–1008.
- [17] A. Chieregato, J.V. Ochoa, C. Bandinelli, G. Fornasari, F. Cavani, M. Mella, ChemSusChem 8 (2015) 398–406.
- [18] Z. Han, X. Li, M. Zhang, Z. Liu, M. Gao, RSC Adv. 5 (2015) 103982–103988.
- [19] C. Angelici, M.E.Z. Velthoorn, B.M. Weckhuysen, P.C.A. Bruijnincx, Catal. Sci. Technol. 5 (2015) 2869–2879.
- [20] O.V. Larina, P.I. Kyriienko, S.O. Soloviev, Catal. Lett. 145 (2015) 1162–1168.

- [21] Y. Sekiguchia, S. Akiyama, W. Urakawa, T. Koyama, A. Miyaji, K. Motokura, T. Baba, *Catal. Commun.* 68 (2015) 20–24.
- [22] T. De Baerdemaeker, M. Feyen, U. Müller, B. Yilmaz, F. Xiao, W. Zhang, T. Yokoi, X. Bao, H. Gies, D.E. De Vos, *ACS Catal.* 5 (2015) 3393–3397.
- [23] M. Zhang, M. Gao, J. Chena, Y. Yu, *RSC Adv.* 5 (2015) 25959–25966.
- [24] R.A.L. Baylona, J. Suna, Y. Wang, *Cat. Today* 259 (2016) 446–452.
- [25] G.O. Ezinkwo, V.F. Tretjakov, R.M. Talyshinsky, A.M. Illobo, T.A. Mutombo, *Catal. Commun.* 43 (2014) 207–212.
- [26] C. Angelici, F. Meirer, M.J. van der Eerden, H.L. Schaink, A. Goryachev, J.P. Hofmann, E.J.M. Hensen, B.M. Weckhuysen, P.C.A. Bruijnincx, *ACS Catal.* 5 (2015) 6005–6015.
- [27] S.-H. Chung, C. Angelici, S. Hinterding, M. Weingarth, M. Baldus, K. Houben, B.M. Weckhuysen, P.C.A. Bruijnincx, *ACS Catal.* 6 (2016) 4034–4045.
- [28] A. Klein, K. Keisers, R. Palkovits, *Appl. Catal. A: Gen.* 514 (2016) 192–202.
- [29] S. Shylesh, A. Gokhale, C. Scown, D. Kim, C. Ho, A.T. Bell, *ChemSusChem* 9 (2016) 1462–1472.
- [30] R. Baylon, J. Sun, Y. Wang, *Cat. Today* 259 (2016) 446–452.
- [31] P. Kyriienko, O. Larina, S. Soloviev, S. Orlyk, S. Dzwigaj, *Catal. Commun.* 77 (2016) 123–126.
- [32] S.V. Lebedev, *Zh. Gen. Khim.* 3 (1933) 698–717.
- [33] A.A. Balandin, *Zh. Fiz. Khim.* 6 (1935) 357–361.
- [34] J. Ostromislenskiy, *J. Russ. Phys. Chem. Soc.* 47 (1915) 1472–1506.
- [35] W. Toussaint, J. Dunn, D. Jackson, *Ind. Eng. Chem.* 39 (1947) 120–125.
- [36] B.B. Corson, H.E. Jones, C.E. Welling, J.A. Hinckley, E.E. Stahly, *Ind. Eng. Chem.* 42 (1950) 359–373.
- [37] W.M. Quattlebaum, W.J. Toussaint, J.T. Dunn, *J. Am. Chem. Soc.* 69 (1947) 593–599.
- [38] G. Natta, R. Rigamonti, *Chim. Ind.* 29 (1947) 195–200.
- [39] S.K. Bhattacharyya, S.K. Sanyal, *J. Catal.* 7 (1967) 152–158.
- [40] O.M. Vinogradova, N.P. Keier, S.Z. Roginskii, *Dokl. Akad. Nauk USSR* 112 (1957) 1075–1078.
- [41] H. Niijyama, S. Morii, E. Echigoya, *Bull. Chem. Soc. Jpn.* 45 (1972) 655–659.
- [42] S. Kvistle, A. Aguero, R.P.A. Sneeden, *Appl. Catal.* 43 (1988) 117–131.
- [43] V. Gruver, A. Sun, J.J. Fripiat, *Catal. Lett.* 34 (1995) 359–364.
- [44] V. Ordovsky, V. Sushkevich, I. Ivanova, US 8921635 (2014).
- [45] V. Ordovsky, V. Sushkevich, I. Ivanova, RU 2440962 (2012).
- [46] S. Hanspal, Z.D. Young, H. Shouand, R.J. Davis, *ACS Catal.* 5 (2015) 1737–1746.
- [47] C. Ledesma, J. Yang, D. Chen, A. Holmen, *ACS Catal.* 4 (2014) 4527–4547.
- [48] V.L. Sushkevich, I.I. Ivanova, E. Taarning, *ChemCatChem* 5 (2013) 2367–2373.
- [49] V.V. Ordovsky, V.L. Sushkevich, I.I. Ivanova, *J. Mol. Catal. A: Gen.* 333 (2010) 85–93.
- [50] D. Palagin, V.L. Sushkevich, I.I. Ivanova, *J. Phys. Chem. C* 120 (2016) 23566–23575.
- [51] J.D. Lewis, S. Van de Vyver, Y. Román-Leshkov, *Angew. Chem. Int. Ed.* 54 (2015) 9835–9838.
- [52] S. Van de Vyver, Y. Román-Leshkov, *Angew. Chem. Int. Ed.* 54 (2015) 12554–12561.
- [53] Y. Wang, J.D. Lewis, Y. Román-Leshkov, *ACS Catal.* 6 (2016) 2739–2744.
- [54] C. Ho, S. Shylesh, A. Bell, *ACS Catal.* 6 (2016) 939–948.
- [55] Z. Young, S. Hanspal, R. Davis, *ACS Catal.* 6 (2016) 3193–3202.
- [56] Y.-P. Li, M. Head-Gordon, A. Bell, *ACS Catal.* 4 (2014) 1537–1545.
- [57] V.L. Sushkevich, I.I. Ivanova, S. Tolborg, E. Taarning, *J. Catal.* 316 (2014) 121–129.
- [58] P. Sykes, *Guidebook to Mechanism in Organic Chemistry*, Longman, London, 1971.
- [59] M. Boronat, A. Corma, M. Renz, *J. Phys. Chem. B* 110 (2006) 21168–21174.